TR 81086

3

ROYAL AIRCRAFT ESTABLISHMENT

*

Technical Report 81086

July 1981

STRESS INTENSITY FACTORS FOR CRACKS AT LOADED HOLES

by

D. P. Rooke
J. Tweed

*

Procurement Executive, Ministry of Defence
Farnborough, Hants

UDC 539.219.2 : 539.4.013.3 : 539.4.014.11

ROYAL AIRCRAFT ESTABLISHMENT

Technical Report 81086

Received for printing 10 July 1981

STRESS INTENSITY FACTORS FOR CRACKS AT LOADED HOLES

by

D. P. Rooke

J. Tweed*

SUMMARY

A method is described for obtaining the opening-mode and sliding-mode stress intensity factors for the tip of a crack at the edge of a circular hole with arbitrary loads on its perimeter. The method involves the solutions of a singular integral equation which arises from expressing the equations of elasticity in terms of Mellin transforms. In developing the method, four particular load distributions are considered: a uniform tensile stress remote from the hole; a point load on the perimeter of the hole; uniform pressure on an arc of the perimeter; a cosine distribution of pressure on the perimeter. It is shown that the stress intensity factor for a short crack is strongly dependent on the distribution of load around the hole; this has important implications for the estimation of fatigue lifetimes. A procedure is indicated for using some of the results to study arbitrary loads on the hole perimeter.

Departmental Reference: Mat 435

* Department of Mathematics, Old Dominion University, VA, USA

LIST OF CONTENTS

1 INTRODUCTION

Cracks in structural components can grow under in-service loads and lead to failure of the component. In order to ensure safety and reliability it is necessary to know both the residual strength of a cracked structure and the rates at which cracks grow in fatigue; both depend upon the stress field at the crack tip, which is characterised by the stress intensity factor.

Because holes are stress concentrators, cracks frequently start at the edges of holes in the structure. Rooke and Tweed[1] have evaluated the opening mode stress intensity factors K_I for cracks at the edges of circular holes in sheets subjected to remote tensile stresses which result in only normal stresses along the crack line; the sliding mode stress intensity factors K_{II} were therefore zero. However, in many practical components the service loads produce shear stresses along the crack line, and a more general method of analysis is required to evaluate the stress intensity factors (K_{II} will now be non-zero, but generally small compared with K_I). Such a method is now available[2,3]; it can be used to obtain both K_I and K_{II} for a crack at the edge of a circular hole in a sheet subjected to arbitrary loading.

In this Report the aim was to model two common practical configurations, namely a crack at the edge of a hole in a sheet subjected to arbitrary loadings remote from the crack, and a crack at a hole subjected to arbitrary loadings on the perimeter of the hole. Four particular load distributions are considered, see Fig 1: they are

(a) a uniform uniaxial tensile stress remote from the crack acting in a direction at an arbitrary angle to the crack line;

(b) a localised radial force at the perimeter of the hole acting at an arbitrary angle to the crack line;

(c) a uniform pressure acting over an arc of the hole perimeter such that the resultant force on the edge of the hole acts in a direction at right angles to the crack line;

(d) a variable pressure (cosine distribution) acting over one half of the hole perimeter such that the resultant force on the edge of the hole acts in a direction at right-angles to the crack line.

Stress intensity factors for cracks in structures subjected to loadings in more than one direction can be obtained from the results for case (a) by using the principle of superposition. The stress intensity factor for the single radial point force in case (b) can be used as a Green's function to obtain results for any arbitrary pressure acting on the hole perimeter. Two particular pressure distributions, cases (c) and (d), have been studied in detail, since these distributions have often been assumed in attempts to model the load transfer in both pin-loaded lugs and fastener holes.

The results obtained in this Report show that the stress intensity factors, K_I and K_{II}, for short cracks depend significantly upon the distribution of loads, even

when the resultant load on the perimeter of the hole is the same. Fatigue lifetimes will therefore be strongly dependent on the load distribution since cracks are short for most of the lifetime.

2 BASIC THEORY

The hole is defined in plane polar co-ordinates (ρ,θ) by $0 \leq \rho < R$ and $0 \leq \theta \leq 2\pi$ and the crack by $R \leq \rho < a$ along $\theta = 0$ (see Fig 1); and the crack length ℓ measured from the edge of the hole is given by $\ell = a - R$. If the component were uncracked, the applied loads would cause stresses $\sigma_{\theta\theta}$ and $\sigma_{\rho\theta}$ along the crack site; which can, in general, be represented as

$$\sigma_{\theta\theta}(\rho,0) = p_0 f_1(r) \quad \text{and} \quad \sigma_{\rho\theta}(\rho,0) = p_0 f_2(r) \tag{1}$$

for $R \leq \rho < a$, where $\sigma_{\theta\theta}$ and $\sigma_{\rho\theta}$ are the normal and shear stresses respectively, $r = \rho/R$, and p_0 is a constant with the dimensions of stress. The loading functions $f_1(r)$ and $f_2(r)$ for the uncracked component are needed to obtain stress intensity factors for the crack component.

It has been shown[2] that K_I and K_{II} can be expressed in terms of two functions $P_1(c)$ and $P_2(c)$, where $c = a/R$, as follows

$$\frac{K_I}{K_0} = -\frac{\sqrt{2}}{(c-1)} P_1(c) \quad \text{and} \quad \frac{K_{II}}{K_0} = -\frac{\sqrt{2}}{(c-1)} P_2(c) \ , \tag{2}$$

where $K_0 = p_0\sqrt{\pi\ell}$. The functions P_1 and P_2 are solutions of the singular integral equations,

$$\frac{1}{\pi}\int_1^c \frac{P_i(t)}{\sqrt{(c-t)(t-1)}} \left\{ \frac{1}{t-r} + k_i(r,t) \right\} dt = -f_i(r), \qquad (1 < r < c) \tag{3}$$

and

$$P_i(1) = 0 \ , \tag{4}$$

for $i = 1$ and 2, where the kernel functions $k_i(r,t)$ are given by,

$$k_1(r,t) = \frac{(1-t^2)^2}{t(1-rt)^3} - \frac{t(1-t^2)}{(1-rt)^2} - \frac{t}{(1-rt)} + \frac{1-t^2}{r^2 t} \tag{5}$$

and

$$k_2(r,t) = \frac{(1-t^2)^2}{t(1-rt)^3} - \frac{(1-t^2)}{t(1-rt)^2} - \frac{t}{(1-rt)} \ . \tag{6}$$

It should be noted that the kernel function $k_1(r,t)$ used to obtain K_I for a loading which is not symmetric about the crack line is identical with the kernel function $k(r,t)$ used in Ref 1 for symmetrical loading. Because of this, K_I for non-symmetrical loadings can be obtained from solutions for symmetrical loadings, see Appendix. There is no equivalent relationship for K_{II}, since K_{II} is identically zero for symmetrical loadings.

The function P_1 is related to the displacement u_θ of the crack surfaces, and P_1 is related to the displacement u_ρ :

$$u_\theta(\rho,0) - u_\theta(\rho,2\pi) = -\frac{4(1-\nu^2)p_0R}{E}\int_r^c \frac{P_1(t)dt}{\sqrt{(c-t)(t-1)}}, \qquad 1 < r < c \tag{7}$$

and

$$u_\rho(\rho,0) - u_\rho(\rho,2\pi) = -\frac{4(1-\nu^2)p_0R}{E}\int_r^c \frac{P_2(t)dt}{\sqrt{(c-t)(t-1)}}, \qquad 1 < r < c \tag{8}$$

where ν is Poisson's ratio and E is Young's modulus.

3 NUMERICAL PROCEDURE

The equations (3) and (4) are reduced to a system of simultaneous linear algebraic equations by using a procedure developed by Erdogan and Gupta[4]. Let

$$u_j = \cos\left[\frac{(2j-1)\pi}{2m}\right] \quad \text{and} \quad v_i = \cos\left[\frac{j\pi}{m}\right], \qquad j = 1,2,\ldots,m ; \tag{9}$$

and let

$$t_k = \tfrac{1}{2}(c-1)u_k + \tfrac{1}{2}(c+1), \qquad k = 1,2,\ldots,m \tag{10}$$

and

$$r_j = \tfrac{1}{2}(c-1)v_j + \tfrac{1}{2}(c+1), \qquad j = 1,2,\ldots,(m-1) . \tag{11}$$

Equations (3) and (4) can now be reduced to the following linear algebraic system:

$$\left.\begin{aligned} \frac{1}{m}\sum_{k=1}^{m} P_i(t_k)\left\{\frac{1}{t_k - r_j} + k_i(r_j,t_k)\right\} &= -f_i(r_j) , \\ \text{and} \qquad \frac{1}{m}\sum_{k=1}^{m} (-1)^k P_i(t_k)\sqrt{\frac{1-u_k}{1+u_k}} &= 0 , \end{aligned}\right\} \tag{12}$$

with $j = 1, 2, \ldots, (m-1)$ and $i = 1, 2$. The solutions $P(t_k)$ of equation (12) are used in a Gauss-Chebyshev interpolation formula to determine the stress intensity factors as follows:

$$\frac{K_i}{K_0} = \frac{\sqrt{3}}{m(c-1)}\sum_{k=1}^{m} (-1)^k\sqrt{\frac{1+u_k}{1-u_k}}\,P_i(t_k) , \qquad i = 1,2 , \tag{13}$$

where for convenience $K_1 = K_I$ and $K_2 = K_{II}$. The number of terms m is chosen large enough to ensure that equation (13) converges and gives values of K_i to the desired accuracy.

4 LOADING FUNCTIONS

In order to obtain the solution to equation (12), the loading functions $f_1(r)$ and $f_2(r)$ must be known. These are obtained from the stress fields along the crack site in the uncracked configuration. In what follows, the stress fields which are considered are due to either uniform applied stresses remote from the crack or radial forces on the hole perimeter. Residual stress fields which may also be present in practical components can be included in $f_1(r)$ and $f_2(r)$. In fact, the residual stress fields which often occur around holes may have a large effect on the stress intensity factor particularly at short crack lengths.

4.1 Uniaxial tensile stress

The stress intensity factors for this configuration have been evaluated[2] by using loading functions obtained from Sokolnikoff[5], *ie* for a uniform uniaxial tensile stress acting at an angle ϕ to the crack line (see Fig 1a)

$$\left.\begin{aligned} f_1(r) &= \tfrac{1}{2}\left(1 + \frac{1}{r^2}\right) - \tfrac{1}{2}\left(1 + \frac{3}{r^4}\right)\cos 2\phi \\ \text{and} \qquad f_2(r) &= \tfrac{1}{2}\left(1 + \frac{2}{r^2} - \frac{3}{r^4}\right)\sin 2\phi \quad . \end{aligned}\right\} \tag{14}$$

In this case the constant p_0 in equation (1) is equal to the applied stress σ .

4.2 Point load

The loading functions needed for a radial force F per unit thickness acting on the hole perimeter at an angle ϕ to the crack line (see Fig 1b) have been derived[2] from the stress functions given by Green and Zerna[6]. The constant p_0 is given by $p_0 = F/(2R)$. The functions can be written as follows:

$$f_1(r) = g_1(r) + \alpha g_2(r) \quad \text{and} \quad f_2(r) = g_3(r) + \alpha g_4(r) \tag{15}$$

where $\alpha = \dfrac{3 - 4\nu}{2(1 - \nu)}$ (plane strain), or $\alpha = \dfrac{3 - \nu}{2}$ (plane stress) . (16)

$$g_1(r) = \frac{1}{\pi}\left[\frac{1}{r^2} + \frac{4}{X^4} - \frac{2r\cos\phi}{X^3} - \frac{(1 + 4r^2 - r^4)\cos\phi}{rX^4}\right] , \tag{17}$$

$$g_2(r) = \frac{1 + r^2}{\pi r^3}\cos\phi \quad , \tag{18}$$

$$g_3(r) = \frac{(1 - r^2)^2}{\pi r X^4}\sin\phi \quad , \tag{19}$$

and

$$g_4(r) = \frac{1 - r^2}{\pi r^3}\sin\phi \quad . \tag{20}$$

where $$X^2 = 1 - 2r\cos\phi + r^2 \quad . \tag{21}$$

If we write

$$\left.\begin{aligned} P_1(t) &= Q_1(t) + \alpha Q_2(t) \\ \text{and} \qquad P_2(t) &= Q_3(t) + \alpha Q_4(t) \quad , \end{aligned}\right\} \tag{22}$$

where $Q_s(s = 1,2,3,4)$ is independent of Poisson's ratio, and introduce the functions

$$\left.\begin{aligned} M_1(r,t) &= M_2(r,t) = \frac{1}{t - r} + k_1(r,t) \\ \text{and} \qquad M_3(r,t) &= M_4(r,t) = \frac{1}{t - r} + k_2(r,t) \quad , \end{aligned}\right\} \tag{23}$$

then equations (3) and (4) are equivalent to

$$\frac{1}{\pi}\int_1^c \frac{Q_s(t)M_s(r,t)}{\sqrt{(c - t)(t - 1)}} = -g_s(r) \quad , \qquad 1 < r < c \tag{24}$$

and

$$Q_s(1) = 0 \tag{25}$$

for $s = 1, 2, 3, 4$. Therefore, by the method of Erdogan and Gupta (see section 3), the linear set of equations to be solved for $Q_s(t)$ is

$$\left.\begin{aligned} \frac{1}{m}\sum_{k=1}^{m} Q_s(t_k)M_s(r_j,t_k) &= -g_s(r_j) \\ \frac{1}{m}\sum_{k=1}^{m} (-1)^k Q_s(t_k)\sqrt{\frac{1 - u_k}{1 + u_k}} &= 0 \quad , \end{aligned}\right\} \tag{26}$$

for $j = 1, 2, \ldots, (m - 1)$ and $s = 1, 2, 3, 4$. The stress intensity factors are given by

$$K_1 = K^{(1)} + \alpha K^{(2)} \quad \text{and} \quad K_2 = K^{(3)} + \alpha K^{(4)} \tag{27}$$

where $$\frac{K^{(s)}}{K_0} = \frac{\sqrt{2}}{m(c - 1)}\sum_{k=1}^{m} (-1)^k \sqrt{\frac{1 + u_k}{1 - u_k}}\, Q_s(t_k) \tag{28}$$

for $s = 1, 2, 3, 4$.

4.3 Arc of uniform pressure

The stress function derived by Green and Zerna[6] has been used[3] to obtain the loading functions $f_1(r)$ and $f_2(r)$ for the case of a hole loaded by a uniform pressure on

an arc of the perimeter; the arc on which the pressure acts subtends an angle 2β at the centre of the hole and is symmetric about the line $\theta = \pi/2$ (see Fig 1c). As in the previous section, we write

$$f_1(r) = g_1(r) + \alpha g_2(r) \quad \text{and} \quad f_2(r) = g_3(r) + \alpha g_4(r) \ , \tag{29}$$

where

$$g_1(r) = \frac{1}{\pi}\left\{\tan^{-1}\left(\frac{\sin 2\beta}{r^2 + \cos 2\beta}\right) + \frac{\beta}{r^2} - \left(r - \frac{1}{r}\right)\left(\frac{1}{r_2^2} - \frac{1}{r_1^2}\right)\frac{\cos\beta}{2}\right\} \ , \tag{30}$$

$$g_2(r) = 0 \ ,$$

$$g_3(r) = \frac{1}{2\pi}\left(r - \frac{1}{r}\right)\left[\frac{r - \sin\beta}{r_2^2} - \frac{r + \sin\beta}{r_1^2}\right] \ , \tag{31}$$

and

$$g_4(r) = \frac{1}{\pi}\left(\frac{1}{r^2} - 1\right)\frac{\sin\beta}{r} \ , \tag{32}$$

with

$$r_1^2 = 1 + 2r\sin\beta + r^2 \quad \text{and} \quad r_2^2 = 1 - 2r\sin\beta + r^2 \ . \tag{33}$$

The stress intensity factors are calculated by following the steps of section 4.2 from equation (22) onwards, but with the following limitation: since $g_2(r) = 0$ then $Q_2(t) = 0$ and $M_2(r,t) = 0$ and hence $K^{(2)} = 0$.

4.4 Cosine distribution of pressure

In this case the pressure $p(\theta)$ is distributed on the perimeter of the hole according to

$$p(\theta) = p_0 \cos\left(\frac{\pi}{2} - \theta\right) = p_0 \sin\theta \ , \quad 0 \leq \theta \leq \pi \ , \tag{34}$$

and is zero otherwise.

The loading functions for any arbitrary distribution of pressure can be derived, using the principle of superposition, from those for a radial force acting on the perimeter (see section 4.2). For the case of a cosine distribution of pressure the loading functions are given[3] by

$$f_1(r) = I_1 + \alpha I_2 \quad \text{and} \quad f_2(r) = I_3 + \alpha I_4 \ , \tag{35}$$

where

$$I_s = \frac{1}{2}\int_0^{\pi} g_s \sin\phi \, d\phi \ , \qquad s = 1,2,3,4 \ ; \tag{36}$$

g_s for $s = 1, 2, 3, 4$ are the loading functions for a point load, given by equations (17) and (20). The integrals I_s are evaluated, for $s = 1, 2, 3, 4$, in Appendix B of Ref 3; the expressions for $f_1(r)$ and $f_2(r)$ become

$$f_1(r) = \frac{1}{2\pi}\left[3 + \frac{1}{r^2} + \left(\frac{1}{2r^3} + \frac{1}{r} - \frac{3r}{2}\right)\ln\left(\frac{r+1}{r-1}\right)\right] \tag{37}$$

and

$$f_2(r) = \frac{\gamma(1 - r^2)}{4r^3} \quad , \tag{38}$$

where $\gamma = \nu - 1$.

With the following definitions,

$$\left.\begin{aligned} h_1(r) &= f_1(r) \quad \text{and} \quad h_2(r) = \frac{1}{\gamma} f_2(r) \\ \text{and} \\ Q_1(r) &= P_1(r) \quad \text{and} \quad Q_2(r) = \frac{1}{\gamma} P_2(r) \quad , \end{aligned}\right\} \tag{39}$$

equations (3) and (4) become

$$\frac{1}{\pi}\int_1^c \frac{Q_i(t)}{\sqrt{(c - t)(t - 1)}}\left\{\frac{1}{t - r} + k_i(r,t)\right\} = - h_i(t) \quad , \qquad 1 < r < c \quad , \tag{40}$$

with $Q_i(1) = 0$, for $i = 1, 2$. The stress intensity factors are given by

$$\frac{K_I}{K_0} = - \frac{\sqrt{2}}{(c - 1)} Q_1(c) \quad \text{and} \quad \frac{K_{II}}{K_0} = - \frac{\gamma\sqrt{2}}{(c - 1)} Q_2(c) \quad . \tag{41}$$

The numerical procedure to solve equation (40) and hence obtain K_I and K_{II} is as outlined in section 3.

5 RESULTS

Solutions of the singular integral equations (3) and (4) in section 2 have been obtained and hence the stress intensity factors evaluated, by using the numerical procedure outlined in section 3 and the loading functions developed in section 4.

5.1 Uniaxial tensile stress

Values of the opening-mode stress intensity factor K_I/K_0 are given in Table 1 as a function of the crack length c/R for various values of the angle ϕ between the direction of the stress and the crack line. The results for ϕ of 0° and 90° agree with those for biaxial and uniaxial stress given in Ref 1. Plots of K_I/K_0 against c/R are shown in Fig 2 for $0^\circ \leq \phi < 90^\circ$. For other values of ϕ the stress intensity factor $K_I(\phi)$ is obtained from the following symmetry relations:

$$K_I(-\phi) = K_I(180^\circ - \phi) = K_I(\phi) \quad , \qquad 0^\circ \leq \phi \leq 180^\circ \quad . \tag{42}$$

Negative values of K_I imply crack closure and are therefore not generally valid but they can be superposed with values for other stress fields provided that the resultant stress field causes the crack to remain open along its whole length.

Values of the sliding-mode stress intensity factor K_{II}/K_0 are given in Table 2 and plotted in Fig 2. The symmetry relations are

$$\left.\begin{aligned} K_{II}(-\phi) &= K_{II}(180^\circ - \phi) = -K_{II}(\phi) \\ \text{and} \qquad K_{II}(90^\circ - \phi) &= K_{II}(\phi) \quad , \qquad 0^\circ \leqslant \phi \leqslant 180^\circ \ . \end{aligned}\right\} \tag{43}$$

5.2 Point load

The components $K^{(1)}/K_0$ and $K^{(2)}/K_0$ of the opening-mode stress intensity factor K_I/K_0 are given in Tables 3 and 4, respectively. Curves of these two components are plotted as a function of ℓ/R in Fig 3 for various values of ϕ. For clarity of presentation $K^{(1)}/K_0$ is plotted for $0^\circ \leqslant \phi \leqslant 180^\circ$ and $K^{(2)}/K_0$ for $90^\circ \leqslant \phi \leqslant 180^\circ$. Results for other values of ϕ can be obtained from the following symmetry relations:

$$\left.\begin{aligned} K^{(1)}(-\phi) &= K^{(1)}(\phi) \\ \text{and} \qquad K^{(2)}(-\phi) &= K^{(2)}(\phi) = -K^{(2)}(180^\circ - \phi) \ , \qquad 0^\circ \leqslant \phi \leqslant 180^\circ \ . \end{aligned}\right\} \tag{44}$$

The components $K^{(3)}/K_0$ and $K^{(4)}/K_0$ of the sliding-mode stress intensity factor K_{II}/K_0 are given in Tables 5 and 6 respectively. These are plotted as a function of ℓ/R in Fig 4 for various values of ϕ. The symmetry relationships are

$$\left.\begin{aligned} K^{(3)}(-\phi) &= -K^{(3)}(\phi) \\ \text{and} \qquad K^{(4)}(180^\circ - \phi) &= K^{(4)}(\phi) = -K^{(4)}(-\phi) \ , \qquad 0^\circ \leqslant \phi \leqslant 180^\circ \ . \end{aligned}\right\} \tag{45}$$

In general K_I and K_{II} are functions of Poisson's ratio ν, for this loading, since from equation (27) we obtain, for plane strain,

$$\left.\begin{aligned} \frac{K_I}{K_0} &= \frac{K^{(1)}}{K_0} + \frac{(3 - 4\nu)}{2(1 - \nu)} \frac{K^{(2)}}{K_0} \\ \text{and} \qquad \frac{K_{II}}{K_0} &= \frac{K^{(3)}}{K_0} + \frac{(3 - 4\nu)}{2(1 - \nu)} \frac{K^{(4)}}{K_0} \ . \end{aligned}\right\} \tag{46}$$

Values of K_I/K_0 and K_{II}/K_0 have been calculated for $\nu = 0.3$ and are shown in Figs 5 and 6 respectively as a function of ℓ/R for various values of the angle ϕ. For $\phi = 90^\circ$ the component $K^{(2)} = 0$ and the opening-mode stress intensity factor is independent of Poisson's ratio, and is one half the value obtained previously[1] for two equal and opposite forces acting on the hole perimeter.

For $\phi \leqslant 15^\circ$ crack closure can occur for some crack lengths, and if it does occur the values of K_I calculated by the present methods are invalid; if closure occurs at the tip K_I will be negative. The values of K_I obtained can be used only if another

stress field is superimposed on that due to the point load, such that the crack faces do not touch at any point along the length of the crack.

5.3 Arc of uniform pressure

Values of the opening-mode stress intensity factor K_I/K_F are given in Tables 7a&b and are plotted in Fig 7 as a function of the angle β for various values of the crack length. The normalising constant K_F is given by

$$K_F = K_0 \sin\beta = p_0\sqrt{\pi\ell}\sin\beta \quad . \tag{47}$$

It is convenient to use K_F since it is proportional to the resultant force $P \sin\beta$ acting on the hole perpendicular to the crack-line. For $\beta = 0^\circ$ the results agree with $K^{(1)}/K_0$ for a point force acting at an angle $\phi = 90^\circ$ to the crack-line (Table 3); for $\beta = 90^\circ$ the values of K_I/K_F are one half of the values obtained previously[1] for a uniform pressure acting over the whole perimeter.

The values of K_I/K_F given in Tables 7a&b and Fig 7 are for $0^\circ \leq \beta \leq 90^\circ$; values for $\beta > 90^\circ$ can be obtained as follows:

$$K_I(\beta) + K_I(180^\circ - \beta) = 2K_I(90^\circ) , \qquad 0^\circ \leq \beta \leq 180^\circ \quad . \tag{48}$$

The two components $K^{(3)}/K_F$ and $K^{(4)}/K_F$ of the sliding-mode stress intensity factor are tabulated in Tables 8a&b; the function $K^{(4)}/K_F$ is a function of crack length only, independent of the angle β . Values of $K^{(3)}/K_F$ are plotted as a function of β , for $0^\circ \leq \beta \leq 90^\circ$, in Fig 8a for various crack lengths. The component $K^{(4)}/K_F$ is plotted in Fig 8b as a function of ℓ/R .

The symmetry relationship for $K^{(3)}$ is as follows:

$$K^{(3)}(\beta) = K^{(3)}(180^\circ - \beta) , \qquad 0^\circ \leq \beta \leq 180^\circ \quad . \tag{49}$$

5.4 Cosine distribution of pressure

Values of K_I/K_F and $\tau^{-1}(K_{II}/K_F)$ are tabulated in Table 9 for the cosine distribution of pressure; for this case K_F is given by

$$K_F = \frac{F}{\pi R}\sqrt{\pi\ell} \tag{50}$$

where F is the resultant force acting perpendicular to the crack-line and is given by

$$F = \frac{+p_0\pi R}{2} \quad . \tag{51}$$

Thus

$$K_F = \frac{+F_0}{\sqrt{\pi\ell}} \quad . \tag{52}$$

The opening-mode stress intensity factor is plotted as K_I/K_F against ℓ/R in Fig 9. Values of K_I/K_F for two other load distributions having the same resultant force perpendicular to the crack-line are also plotted in Fig 9; the two distributions are a point force acting at an angle $\phi = 90^o$ (see Fig 5) and a uniform pressure acting on a semi-circular arc of the perimeter (see Fig 7). Comparison of these three curves shows that although the resultant force is the same, the different load distributions lead to differences in the stress intensity factors, and these differences are greatest when the cracks are short.

Fig 9 also shows a plot of $\gamma^{-1}K_{II}/K_F$ against ℓ/R .

6 DISCUSSION

The method described in this Report has two main advantages; it is efficient in computing requirements and it is accurate at short crack lengths. The largest number of simultaneous linear equations needed to obtain results accurate to ~0.1% was 24. Hsu[7] who has solved the crack problem for uniaxial tensile stress only (see Fig 1a) required between two and six times as many equations. His method which uses conformal mapping techniques becomes less accurate for short cracks, in contrast to the present method for which the stress intensity factor tends towards the correct limit, for a crack at the edge of a hole, as ℓ/R tends to zero. This ensures that values of stress intensity factors are accurate for short cracks, and this is a necessary requirement for the estimation of fatigue lifetimes to be reliable.

This limiting value can be expressed in terms of the loading functions,

$$\lim_{\ell/R\to 0}\{K_I\} = 1.122c_{\theta\theta}(1,0)\sqrt{\pi\ell} = 1.122p_0 f_1(1)\sqrt{\pi\ell} \qquad (53)$$

where the factor 1.122 is the usual edge correction factor. It therefore follows from the definition of $K_0 (= p_0\sqrt{\pi\ell})$ that

$$\lim_{\ell/R\to 0}\left\{\frac{K_I}{K_0}\right\} = 1.122f_1(1) \quad . \qquad (54)$$

For a point force ($\phi = 90^o$), $f_1(1) = 2/\pi$ from equations (15), (17) and (21); for an arc of pressure ($\beta = 90^o$), $f_1(1) = 1/2$ from equations (29) and (30); and for a cosine distribution of pressure, $f_1(1) = 2/\pi$ from equation (37).

Comparison of the stress intensity factors for the point force, the arc of pressure and cosine distribution of loads shows (see Fig 9) that the limiting values of K_I/K_F are $1.122 \times (2/\pi)$, $1.122 \times (1/2)$ and $1.122 \times (8/\pi^2)$ respectively; they are in the ratios $1 : 0.78 : 1.27$. Thus even when the three load distributions have the same resultant force F , the values of K_I for short cracks differ significantly from each other. Because of this the precise load distribution must be known if practical estimates of fatigue life and residual strength are to be accurate. This is particularly

important in the calculation of fatigue life because the growth-rate of cracks in fatigue is proportional to K^n where n is of order 2 to 4.

It is most important that the load distribution near the root of the crack is known precisely, since small changes in load in this region result in large changes in K . This can be seen from Figs 5 and 6 where both K_I and K_{II} change rapidly as the angle ϕ between the force and the crack becomes small. A similar effect is seen in Figs 7 and 8, where rapid changes occur at small crack lengths, as the arc over which the uniform pressure acts approaches the crack ($\beta = 90^o$).

The stress intensity factors K_I and K_{II}, obtained in this Report are for a single crack at the edge of a hole with an arbitrary distribution of load on the hole perimeter. Values of the K_I only, for two cracks of unequal length at $\theta = 0$ and π, can be obtained for arbitrary loads by using the principle of superposition (see Appendix) and the method developed in Ref 1. A second, more approximate method[1], can also be used for obtaining K_I for two cracks from that for one crack provided that the load distributions on the perimeter is symmetric about $\theta = \pi/2$. Although only the opening-mode stress intensity factor can be obtained from both procedures this is often adequate for practical structures, since K_I is usually much more than $|K_{II}|$ and the fracture behaviour is dominated by the opening-mode.

The method used in this Report to evaluate stress intensity factors for the four particular loading distributions shown in Fig 1, can be extended to any arbitrary loading on the hole perimeter by a technique using Green's functions[7]. This technique was used in section 4.4 to obtain the loading functions $f_1(r)$ and $f_2(r)$ for the cosine distribution of pressure. For an arbitrary pressure distribution $p(\theta)$ on the hole perimeter, which can be written as

$$p(\theta) = p_0 h(\theta) \quad , \tag{55}$$

equations (35) and (36) become

$$f_1(r) = I_1 + \alpha I_2 \quad \text{and} \quad f_2(r) = I_3 + \alpha I_4 \tag{56}$$

where

$$I_s = \frac{1}{2}\int_0^{2\pi} g_s(\phi) h(\phi) d\phi \quad ; \tag{57}$$

the Green's functions $g_s(\phi)$, for $s = 1, 2, 3$ and 4, are the loading functions for a point load, and are given by equations (17) to (20). After evaluation of I_s, analytically or numerically, the procedure of section 3 can be followed to obtain the stress intensity factors.

The stress intensity factors, obtained in section 5.2 for a point load, may be used directly as Green's functions[7]. Let the force acting on the perimeter between $\theta = \phi$ and $\theta = \phi + d\phi$ due to the pressure $p(\theta)$ be $dF(\phi)$; it is given by

$$dF(\phi) = p(\phi) R d\phi \quad . \tag{58}$$

Let the stress intensity factor (I or II) due to $dF(\phi)$ be $dK(\phi)$; it is given by

$$dK(\phi) = K^u(\phi)dF(\phi) \quad , \tag{59}$$

where $K^u(\phi)$ is the factor for a unit force acting at $\theta = \phi$. Since in general the stress intensity factor is proportional to the applied force F it follows that

$$K^u(\phi) = F^{-1}K^F(\phi) \tag{60}$$

where $K^F(\phi)$ is the factor for a force F acting on the hole perimeter at $\theta = \phi$.

Equation (54) can be written

$$K^u(\phi) = \frac{K^F(\phi)}{F} = \frac{\sqrt{\pi \ell}}{2R}\frac{K^F(\phi)}{\frac{F}{2R\sqrt{\pi \ell}}} = \frac{\sqrt{\pi \ell}}{2R}\left(\frac{K^F(\phi)}{K_0}\right) \tag{61}$$

where $(K^F(\phi)/K_0)$ can be either K_I/K_0 or K_{II}/K_0 obtained in section 5.2.

The principle of superposition states that the stress intensity factor K^p due to $p(\phi)$ for all ϕ is given by summing all the $dK(\phi)$'s, i.e.

$$K^p = \int_0^{2\pi} dK(\phi) \quad . \tag{62}$$

Substitution of equations (55) and (58) to (61) into equation (62) gives

$$K^p = \tfrac{1}{2}p_0\sqrt{\pi \ell}\int_0^{2\pi}\left(\frac{K^F(\phi)}{K_0}\right)h(\phi)d\phi \quad . \tag{63}$$

Thus $(K^F(\phi)/K_0)$ is the Green's function for the stress intensity factor for an arbitrary distribution of pressure and can be obtained from the results for a single point force. The integral in equation (63) will, in general, have to be evaluated numerically. If the loading distribution is determined experimentally so that $h(\phi)$ is known only at discrete points, then the integral in equation (63) would be replaced by an appropriate summation. In order to ensure accurate results, particular care must be taken when ϕ is near zero as $K^F(\phi)$ varies rapidly (see Figs 5 and 6).

7 CONCLUSIONS

(1) A transform method has been developed for obtained opening-mode and sliding-mode stress intensity factors for a crack at the edge of a circular hole; the method is both accurate and efficient in computer usage. The method was developed so that

(a) the stress intensity factor for an arbitrary distribution of pressure in the hole can be obtained from results for a radial point force;

(b) both externally applied loads and residual stress fields can be considered;

(c) it can be extended to calculate opening-mode stress intensity factors for two cracks.

(2) Application of the method to a short crack at the edge of a hole, showed that the stress intensity factor varies significantly with small changes of load distribution on the hole, even if the total load on the hole is the same; this implies that estimates of fatigue lifetimes may be seriously in error, unless the load distribution in the structural component is known accurately.

Appendix

RELATIONSHIP BETWEEN STRESS INTENSITY FACTORS FOR SYMMETRIC AND NON-SYMMETRIC LOAD DISTRIBUTIONS

(see section 2)

By using the principle of superposition, any load distribution which is symmetric with respect to the crack line can be represented as the sum of two asymmetric loadings. In Fig 10, configuration A represents a hole with a crack at its edge along the $\theta = 0$ axis; the hole is loaded symmetrically about the crack line, so that the pressure p^A on the perimeter is given by

$$\left.\begin{aligned} p^A &= p(\theta) \quad , && 0 \leq \theta \leq \pi \\ \text{and} \qquad p^A &= p(-\theta) \quad , && 0 \geq \theta \geq -\pi \quad . \end{aligned}\right\} \tag{A-1}$$

Configuration B represents a similar hole and crack with loading for $0 \leq \theta \leq \pi$ only, so that the pressure p^B on the perimeter is given by

$$\left.\begin{aligned} p^B &= p(\theta) \quad , && 0 \leq \theta \leq \pi \\ \text{and} \qquad p^B &= 0 \quad , && 0 > \theta > -\pi \quad . \end{aligned}\right\} \tag{A-2}$$

Configuration C also represents a similar hole and crack, but is loaded for $0 \geq \theta \geq -\pi$ only, so that the pressure p^C on the perimeter is given by

$$\left.\begin{aligned} p^C &= 0 \quad , && 0 < \theta < \pi \\ \text{and} \qquad p^C &= p(-\theta) \quad , && 0 \geq \theta \geq -\pi \quad . \end{aligned}\right\} \tag{A-3}$$

The stress intensity factors for these three configurations can be written as follows:

$$\text{for A} \qquad K_I = K_I^A \quad \text{and} \quad K_{II} = K_{II}^A \quad ; \tag{A-4}$$

$$\text{for B} \qquad K_I = K_I^B \quad \text{and} \quad K_{II} = K_{II}^B \quad ; \tag{A-5}$$

$$\text{for C} \qquad K_I = K_I^C \quad \text{and} \quad K_{II} = K_{II}^C \quad ; \tag{A-6}$$

From the principle of superposition it follows that

$$\left.\begin{aligned} K_I^A &= K_I^B + K_I^C \\ \text{and} \qquad K_{II}^A &= K_{II}^B + K_{II}^C \quad . \end{aligned}\right\} \tag{A-7}$$

From symmetry considerations it follows that

$$K_I^B = K_I^C \quad \text{and} \quad K_{II}^B = -K_{II}^C \quad ; \tag{A-8}$$

hence

$$\left.\begin{aligned} K_I^B &= K_I^C = \tfrac{1}{2}K_I^A \\ \text{and} \qquad K_{II}^A &= 0 \ . \end{aligned}\right\} \tag{A-9}$$

Thus it follows from equation (A-9) that the opening-mode stress intensity factor K_I for an asymmetric distribution of loads can be obtained from K_I for a symmetric distribution; but, this is not so for K_{II} since it is identically zero for symmetric loadings.

Because this argument applies to configurations with one crack (along $\theta = 0$) or two cracks (along $\theta = 0$ and $\theta = \pi$), the method developed previously[1], for obtaining K_I for two symmetrically loaded cracks of unequal length, can be used to obtain K_I for asymmetrical loadings. The factor K_{II} cannot be determined in this way; but for many practical loadings $|K_{II}| \ll K_I$, so that the fracture of the cracked component is dominated by the opening-mode stress intensity factor.

Table 1

OPENING-MODE STRESS INTENSITY FACTOR K_I/K_0 FOR A CRACK AT THE EDGE OF A HOLE: UNIAXIAL TENSILE STRESS

ℓ/R \ ϕ	0°	15°	30°	45°	60°	75°	90°
0.01	-1.080	-0.787	0.013	1.106	2.199	2.999	3.292
0.02	-1.040	-0.755	0.026	1.092	2.158	2.938	3.224
0.04	-0.967	-0.695	0.049	1.065	2.081	2.824	3.096
0.07	-0.869	-0.615	0.080	1.028	1.976	2.670	2.924
0.10	-0.783	-0.545	0.106	0.994	1.883	2.534	2.772
0.15	-0.664	-0.448	0.141	0.946	1.750	2.339	2.555
0.20	-0.567	-0.370	0.169	0.904	1.639	2.177	2.374
0.30	-0.421	-0.253	0.207	0.836	1.464	1.924	2.092
0.40	-0.320	-0.172	0.232	0.783	1.334	1.737	1.885
0.50	-0.247	-0.115	0.247	0.740	1.234	1.595	1.728
0.60	-0.194	-0.073	0.256	0.706	1.155	1.484	1.605
0.80	-0.123	-0.019	0.265	0.652	1.040	1.323	1.427
1.00	-0.080	0.013	0.266	0.613	0.959	1.213	1.306
1.50	-0.030	0.048	0.260	0.549	0.838	1.050	1.127
2.00	-0.010	0.059	0.250	0.510	0.770	0.961	1.031
3.00	0.002	0.064	0.234	0.466	0.698	0.868	0.930
4.00	0.005	0.063	0.223	0.441	0.659	0.819	0.878
5.00	0.005	0.061	0.215	0.425	0.635	0.789	0.846
6.00	0.005	0.060	0.210	0.414	0.619	0.769	0.824
8.00	0.004	0.057	0.202	0.400	0.598	0.743	0.796
10.00	0.003	0.055	0.197	0.391	0.585	0.727	0.779
20.00	0.002	0.051	0.187	0.373	0.559	0.695	0.744

Table 2

SLIDING-MODE STRESS INTENSITY FACTOR K_{II}/K_0 FOR A CRACK AT THE EDGE OF A HOLE: UNIAXIAL TENSILE STRESS

ℓ/R \ ϕ	0^o	15^o	30^o	45^o
0.01	0.000	0.013	0.023	0.027
0.02	0.000	0.026	0.045	0.052
0.04	0.000	0.050	0.086	0.100
0.07	0.000	0.081	0.141	0.163
0.10	0.000	0.109	0.189	0.218
0.15	0.000	0.147	0.255	0.295
0.20	0.000	0.178	0.308	0.356
0.30	0.000	0.223	0.386	0.446
0.40	0.000	0.252	0.437	0.504
0.50	0.000	0.271	0.470	0.543
0.60	0.000	0.284	0.492	0.568
0.80	0.000	0.297	0.514	0.593
1.00	0.000	0.300	0.520	0.600
1.50	0.000	0.294	0.510	0.589
2.00	0.000	0.283	0.490	0.566
3.00	0.000	0.263	0.455	0.525
4.00	0.000	0.248	0.429	0.496
5.00	0.000	0.237	0.411	0.474
6.00	0.000	0.229	0.397	0.458
8.00	0.000	0.216	0.374	0.432
10.00	0.000	0.209	0.362	0.418
20.00	0.000	0.194	0.336	0.388

Table 3

$K^{(1)}/K_0$ COMPONENT OF THE OPENING-MODE STRESS INTENSITY FACTOR FOR A CRACK AT THE EDGE OF A HOLE: POINT LOAD

ℓ/R \ ϕ	15^o	30^o	45^o	60^o	75^o	90^o	120^o	180^o
0.01	0.579	0.672	0.690	0.696	0.698	0.700	0.701	0.702
0.02	0.448	0.632	0.666	0.678	0.684	0.687	0.690	0.691
0.03	0.323	0.593	0.644	0.661	0.669	0.674	0.678	0.680
0.04	0.205	0.555	0.621	0.645	0.656	0.661	0.667	0.670
0.06	-0.009	0.483	0.579	0.613	0.629	0.638	0.646	0.650
0.08	-0.190	0.417	0.540	0.584	0.604	0.615	0.626	0.631
0.10	-0.339	0.355	0.503	0.556	0.581	0.594	0.607	0.614
0.15	-0.583	0.222	0.420	0.493	0.528	0.547	0.565	0.574
0.20	-0.688	0.118	0.349	0.439	0.482	0.506	0.529	0.540
0.30	-0.688	-0.021	0.238	0.350	0.406	0.437	0.468	0.484
0.40	-0.601	-0.096	0.160	0.282	0.346	0.383	0.419	0.438
0.60	-0.437	-0.148	0.065	0.188	0.259	0.302	0.347	0.371
0.80	-0.311	-0.150	0.017	0.129	0.200	0.245	0.295	0.322
1.00	-0.265	-0.140	-0.008	0.091	0.159	0.204	0.255	0.285
1.50	-0.179	-0.111	-0.031	0.041	0.098	0.139	0.190	0.221
2.00	-0.138	-0.091	-0.035	0.020	0.066	0.103	0.150	0.181
3.00	-0.097	-0.068	-0.034	0.002	0.036	0.064	0.104	0.133
4.00	-0.076	-0.056	-0.031	-0.004	0.022	0.043	0.079	0.105
6.00	-0.054	-0.041	-0.025	-0.008	0.010	0.026	0.053	0.074
8.00	-0.043	-0.033	-0.021	-0.008	0.005	0.018	0.039	0.057
10.00	-0.035	-0.028	-0.018	-0.008	0.003	0.013	0.031	0.046
20.00	-0.019	-0.016	-0.011	-0.006	-0.000	0.005	0.015	0.023

Table 4

$K^{(2)}/K_0$ COMPONENT OF THE OPENING-MODE STRESS INTENSITY FACTOR FOR A CRACK AT THE EDGE OF A HOLE: POINT LOAD

s / s/R	15°	30°	45°	60°	75°	90°	180°
0.01	0.676	0.606	0.495	0.350	0.181	0.000	-0.700
0.02	0.663	0.595	0.486	0.343	0.178	0.000	-0.687
0.03	0.651	0.584	0.477	0.337	0.175	0.000	-0.674
0.04	0.639	0.573	0.468	0.331	0.171	0.000	-0.662
0.06	0.617	0.553	0.452	0.319	0.165	0.000	-0.639
0.08	0.596	0.534	0.436	0.309	0.160	0.000	-0.617
0.10	0.577	0.517	0.422	0.298	0.155	0.000	-0.597
0.15	0.533	0.478	0.390	0.276	0.143	0.000	-0.552
0.20	0.496	0.445	0.363	0.257	0.133	0.000	-0.514
0.30	0.436	0.391	0.319	0.226	0.117	0.000	-0.451
0.40	0.389	0.349	0.285	0.202	0.104	0.000	-0.403
0.60	0.322	0.288	0.235	0.166	0.086	0.000	-0.333
0.80	0.275	0.246	0.201	0.142	0.074	0.000	-0.284
1.00	0.240	0.215	0.176	0.124	0.064	0.000	-0.249
1.50	0.184	0.165	0.135	0.095	0.049	0.000	-0.191
2.00	0.150	0.134	0.110	0.078	0.040	0.000	-0.155
3.00	0.110	0.099	0.081	0.057	0.030	0.000	-0.114
4.00	0.087	0.078	0.064	0.045	0.023	0.000	-0.090
6.00	0.063	0.056	0.045	0.032	0.017	0.000	-0.064
8.00	0.048	0.043	0.035	0.025	0.013	0.000	-0.050
10.00	0.039	0.035	0.029	0.020	0.011	0.000	-0.041
20.00	0.021	0.019	0.015	0.011	0.006	0.000	-0.021

Table 5

$K^{(3)}/K_0$ COMPONENT OF THE SLIDING-MODE STRESS INTENSITY FACTOR FOR A CRACK AT THE EDGE OF A HOLE: POINT LOAD

β / ℓ/R	15^0	30^0	45^0	60^0	75^0	90^0	120^0
0.01	0.004	0.000	0.000	0.000	0.000	0.000	0.000
0.02	0.014	0.002	0.000	0.000	0.000	0.000	0.000
0.03	0.031	0.004	0.001	0.001	0.000	0.000	0.000
0.04	0.054	0.007	0.002	0.001	0.000	0.000	0.000
0.06	0.113	0.015	0.004	0.002	0.001	0.001	0.000
0.08	0.185	0.025	0.008	0.003	0.002	0.001	0.000
0.10	0.263	0.038	0.011	0.005	0.003	0.001	0.001
0.15	0.454	0.074	0.023	0.010	0.005	0.003	0.001
0.20	0.606	0.114	0.037	0.016	0.008	0.005	0.002
0.30	0.762	0.190	0.067	0.030	0.016	0.009	0.004
0.40	0.787	0.248	0.095	0.044	0.024	0.014	0.006
0.60	0.703	0.307	0.138	0.070	0.039	0.023	0.009
0.80	0.595	0.318	0.163	0.088	0.051	0.031	0.013
1.00	0.505	0.306	0.173	0.100	0.060	0.038	0.016
1.50	0.332	0.257	0.171	0.111	0.072	0.048	0.022
2.00	0.264	0.211	0.155	0.109	0.075	0.052	0.025
3.00	0.170	0.150	0.123	0.095	0.071	0.053	0.027
4.00	0.122	0.114	0.099	0.081	0.064	0.049	0.027
6.00	0.075	0.075	0.070	0.061	0.052	0.042	0.025
8.00	0.053	0.053	0.053	0.049	0.042	0.036	0.022
10.00	0.040	0.043	0.043	0.040	0.036	0.031	0.020
20.00	0.016	0.019	0.021	0.021	0.020	0.018	0.013

Table 6

$K^{(4)}/K_0$ COMPONENT OF THE SLIDING-MODE STRESS INTENSITY FACTOR FOR A CRACK AT THE EDGE OF A HOLE: POINT LOAD

ℓ/R \ ϕ	15°	30°	45°	60°	75°	90°
0.01	-0.001	-0.002	-0.003	-0.004	-0.004	-0.004
0.02	-0.002	-0.004	-0.006	-0.007	-0.008	-0.008
0.03	-0.003	-0.006	-0.009	-0.011	-0.012	-0.012
0.04	-0.004	-0.008	-0.011	-0.014	-0.016	-0.016
0.06	-0.006	-0.012	-0.016	-0.020	-0.022	-0.023
0.08	-0.008	-0.015	-0.021	-0.026	-0.029	-0.030
0.10	-0.009	-0.018	-0.025	-0.031	-0.035	-0.036
0.15	-0.013	-0.025	-0.035	-0.043	-0.048	-0.049
0.20	-0.016	-0.030	-0.043	-0.052	-0.058	-0.060
0.30	-0.020	-0.039	-0.054	-0.067	-0.074	-0.077
0.40	-0.023	-0.044	-0.063	-0.077	-0.085	-0.089
0.60	-0.026	-0.051	-0.072	-0.088	-0.098	-0.102
0.80	-0.028	-0.054	-0.076	-0.093	-0.104	-0.107
1.00	-0.028	-0.054	-0.077	-0.094	-0.105	-0.109
1.50	-0.027	-0.052	-0.074	-0.091	-0.101	-0.105
2.00	-0.025	-0.049	-0.069	-0.084	-0.094	-0.097
3.00	-0.021	-0.041	-0.058	-0.071	-0.080	-0.082
4.00	-0.018	-0.035	-0.050	-0.061	-0.068	-0.071
6.00	-0.014	-0.027	-0.038	-0.047	-0.052	-0.054
8.00	-0.011	-0.022	-0.031	-0.038	-0.043	-0.044
10.00	-0.010	-0.018	-0.026	-0.032	-0.036	-0.037
20.00	-0.005	-0.010	-0.014	-0.018	-0.020	-0.020

Table 7a

OPENING-MODE STRESS INTENSITY FACTOR K_I/K_F FOR A CRACK AT THE EDGE OF A HOLE: ARC OF UNIFORM PRESSURE

β / t/R	0°	15°	30°	45°	60°	67°	75°
0.01	0.700	0.706	0.733	0.776	0.843	0.884	0.938
0.02	0.687	0.695	0.718	0.760	0.824	0.862	0.910
0.05	0.649	0.656	0.676	0.715	0.769	0.799	0.830
0.10	0.594	0.600	0.618	0.649	0.689	0.707	0.716
0.15	0.547	0.552	0.567	0.592	0.621	0.630	0.624
0.20	0.506	0.510	0.522	0.542	0.562	0.565	0.550
0.30	0.437	0.440	0.449	0.460	0.468	0.463	0.443
0.50	0.338	0.340	0.348	0.346	0.342	0.334	0.318
0.70	0.271	0.272	0.275	0.272	0.265	0.258	0.247
1.00	0.204	0.204	0.203	0.201	0.194	0.190	0.184
1.50	0.139	0.139	0.138	0.135	0.131	0.129	0.127
2.00	0.103	0.102	0.101	0.099	0.097	0.097	0.096
3.00	0.064	0.064	0.063	0.062	0.062	0.062	0.062
5.00	0.034	0.034	0.033	0.033	0.033	0.033	0.033
9.00	0.015	0.015	0.015	0.015	0.015	0.015	0.016

Table 7b

OPENING-MODE STRESS INTENSITY FACTOR K_I/K_F FOR A CRACK AT THE EDGE OF A HOLE: ARC OF UNIFORM PRESSURE

β / t/R	80°	85°	87°	89°	89.5°	90°
0.01	0.974	1.000	0.990	0.876	0.757	0.550
0.02	0.937	0.940	0.904	0.740	0.647	0.540
0.05	0.836	0.789	0.720	0.590	0.550	0.510
0.10	0.698	0.626	0.570	0.502	0.485	0.468
0.15	0.596	0.530	0.493	0.452	0.442	0.432
0.20	0.521	0.467	0.441	0.414	0.407	0.400
0.30	0.418	0.385	0.370	0.356	0.352	0.349
0.50	0.304	0.289	0.284	0.278	0.277	0.276
0.70	0.240	0.232	0.230	0.227	0.226	0.226
1.00	0.181	0.178	0.177	0.176	0.176	0.176
1.50	0.127	0.126	0.126	0.126	0.125	0.125
2.00	0.096	0.095	0.096	0.096	0.096	0.096
3.00	0.062	0.062	0.062	0.062	0.062	0.062
5.00	0.033	0.034	0.034	0.034	0.034	0.034
9.00	0.016	0.016	0.016	0.016	0.016	0.016

Table 8a

$K^{(3)}/K_F$ COMPONENT OF THE SLIDING-MODE STRESS INTENSITY FACTOR FOR A CRACK AT THE EDGE OF A HOLE: ARC OF UNIFORM PRESSURE

β / t/R	0°	15°	30°	45°	60°	67°	75°
0.01	0.000	0.000	0.000	0.000	0.000	0.000	0.000
0.02	0.000	0.000	0.000	0.000	0.000	0.000	0.001
0.05	0.000	0.000	0.001	0.001	0.002	0.003	0.006
0.10	0.001	0.002	0.002	0.003	0.006	0.009	0.019
0.15	0.001	0.003	0.004	0.006	0.011	0.018	0.036
0.20	0.003	0.005	0.006	0.009	0.018	0.028	0.054
0.30	0.009	0.010	0.012	0.017	0.032	0.047	0.083
0.50	0.019	0.020	0.024	0.034	0.056	0.077	0.116
0.70	0.026	0.028	0.035	0.047	0.073	0.094	0.129
1.00	0.033	0.040	0.046	0.060	0.085	0.104	0.132
1.50	0.040	0.050	0.056	0.069	0.090	0.102	0.123
2.00	0.042	0.055	0.060	0.070	0.087	0.095	0.112
3.00	0.041	0.054	0.058	0.065	0.076	0.081	0.091
5.00	0.035	0.040	0.048	0.052	0.058	0.060	0.066
9.00	0.033	0.033	0.034	0.036	0.038	0.039	0.042

Table 8b

$K^{(3)}/K_F$ AND $K^{(4)}/K_F$ COMPONENT OF THE SLIDING-MODE STRESS INTENSITY FACTOR FOR A CRACK AT THE EDGE OF A HOLE: ARC OF UNIFORM PRESSURE

β / t/R	80°	85°	87°	89°	89.5°	90°	$K^{(4)}/K_F$ all β
0.01	0.001	0.002	0.006	0.044	0.114	0.354	-0.004
0.02	0.002	0.008	0.021	0.113	0.202	0.351	-0.008
0.05	0.012	0.041	0.087	0.220	0.277	0.344	-0.020
0.10	0.039	0.103	0.165	0.266	0.298	0.332	-0.036
0.15	0.067	0.145	0.201	0.277	0.298	0.321	-0.049
0.20	0.092	0.170	0.218	0.278	0.294	0.311	-0.060
0.30	0.125	0.194	0.230	0.270	0.281	0.292	-0.077
0.50	0.153	0.201	0.224	0.248	0.254	0.260	-0.096
0.70	0.158	0.194	0.210	0.226	0.231	0.235	-0.105
1.00	0.153	0.178	0.188	0.200	0.202	0.205	-0.109
1.50	0.137	0.152	0.159	0.166	0.168	0.169	-0.105
2.00	0.121	0.132	0.137	0.142	0.143	0.144	-0.097
3.00	0.097	0.104	0.107	0.110	0.111	0.111	-0.082
5.00	0.069	0.073	0.074	0.076	0.076	0.076	-0.061
9.00	0.042	0.043	0.044	0.044	0.044	0.044	-0.040

Table 9

OPENING AND SLIDING-MODE STRESS INTENSITY FACTORS FOR A CRACK AT THE EDGE OF A HOLE: COSINE DISTRIBUTION OF PRESSURE

ℓ/R	K_I/K_F	$K_{II}/(\gamma K_F)$
0.01	0.869	-0.004
0.02	0.837	-0.008
0.05	0.760	-0.020
0.10	0.663	-0.036
0.15	0.589	-0.049
0.20	0.530	-0.060
0.30	0.440	-0.077
0.50	0.325	-0.096
0.70	0.255	-0.105
1.00	0.190	-0.109
2.00	0.097	-0.097
3.00	0.062	-0.082
5.00	0.034	-0.061
9.00	0.016	-0.040

LIST OF SYMBOLS

a	half of total crack length
c	$= a/R$
E	Young's modulus
F	for per unit thickness
$dF(\phi)$	force acting between ϕ and $\phi + d\phi$
f_i	loading functions $(i = 1,2)$
g_i	components of loading functions $(i = 1,2,3,4)$
h_1, h_2	functions defined by equation (39)
$h(\theta)$	pressure distribution on the perimeter of a hole
I_i	integrals defined by equation (36)
P_1, P_2	functions defined by equations (7) and (8)
p_0	constant pressure (or stress)
j, k	summation variables
k_1, k_2	functions defined by equations (5) and (6)
K_0	stress intensity factor SIF $(= p_0\sqrt{\pi\ell})$
K_I	opening-mode SIF
K_{II}	sliding-mode SIF
K_1, K_2	K_I and K_{II} respectively
$K^{(i)}$	components of SIF $(i = 1,2,3,4)$ - see equation (27)
K_F	SIF due to resultant force
$dK(\phi)$	SIF due to $dF(\phi)$
$K^u(\phi)$	SIF due to unit force at ϕ
$K^F(\phi)$	SIF due to force F at ϕ
K^p	SIF due to arbitrary distribution of pressure
ℓ	$= a - R$
m	number of simultaneous equations
M_i	functions defined by equation (23), $(i = 1,2,3,4)$
Q_i	functions defined by equation (22), $(i = 1,2,3,4)$
R	radius of circular hole
r	$= \rho/R$
r_j	discrete value of r

LIST OF SYMBOLS (concluded)

r_1^2, r_2^2	functions defined by equation (33)
t	variable of integration
t_k	discrete value of t
u_θ	angular displacement
u_ρ	radial displacement
X	function defined by equation (21)
α	$= (3 - 4\nu)/[2(1 - \nu)]$ or $(3 - \nu)/2$
β	angle (section 4.3)
γ	$\alpha - 1$
θ	polar co-ordinate
ν	Poisson's ratio
ρ	polar co-ordinate
σ	applied stress
$\sigma_{\theta\theta}$	normal stress
$\sigma_{\rho\theta}$	shear stress
ϕ	angle between force and crack line

REFERENCES

No.	Author	Title, etc
1	D.P. Rooke J. Tweed	Opening-mode stress intensity factors for two unequal cracks at a hole. RAE Technical Report 79105 (1979)
2	J. Tweed D.P. Rooke	The stress intensity factor for a crack at the edge of a loaded hole. *Int. J. Solids Structures*, 15, 899-906 (1979)
3	D.P. Rooke J. Tweed	Stress intensity factors for a crack at the edge of a pressurized hole. *Int. J. Engng. Sci.*, 18, 109-121 (1980)
4	F. Erdogan G.D. Gupta	On the numerical solution of singular integral equations. *Quart. Appl. Maths.*, 29, 525-534 (1972)
5	I.S. Sokolnikoff	*Mathematical theory of elasticity*, 2nd Edition p 291, New York, McGraw-Hill (1956)
6	A.E. Green W. Zerna	*Theoretical elasticity*, 2nd Edition, p 285, Oxford, Clarendon Press (1968)
7	D.J. Cartwright D.P. Rooke	Green's functions in fracture mechanics, in *Fracture mechanics: current status, future prospects*. Edited by R.A. Smith, pp 91-123, London, Pergamon (1979) RAE Technical Report 80035 (1980)

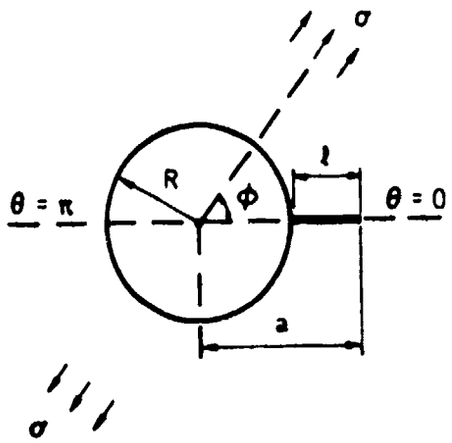

a Uniaxial tensile stress σ remote from hole

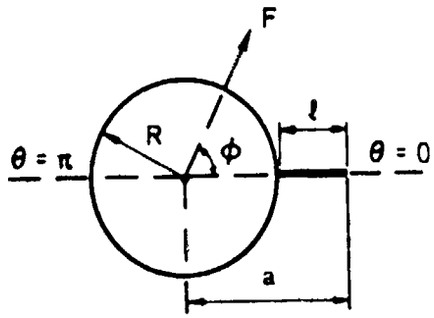

b Localized force P on hole perimeter

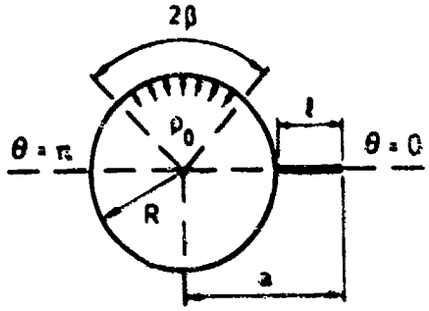

c Uniform pressure on an arc of the hole perimeter

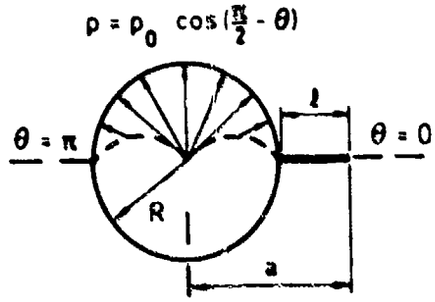

d Cosine distribution of pressure on hole perimeter

Fig 1a-d Load distributions

Fig 2

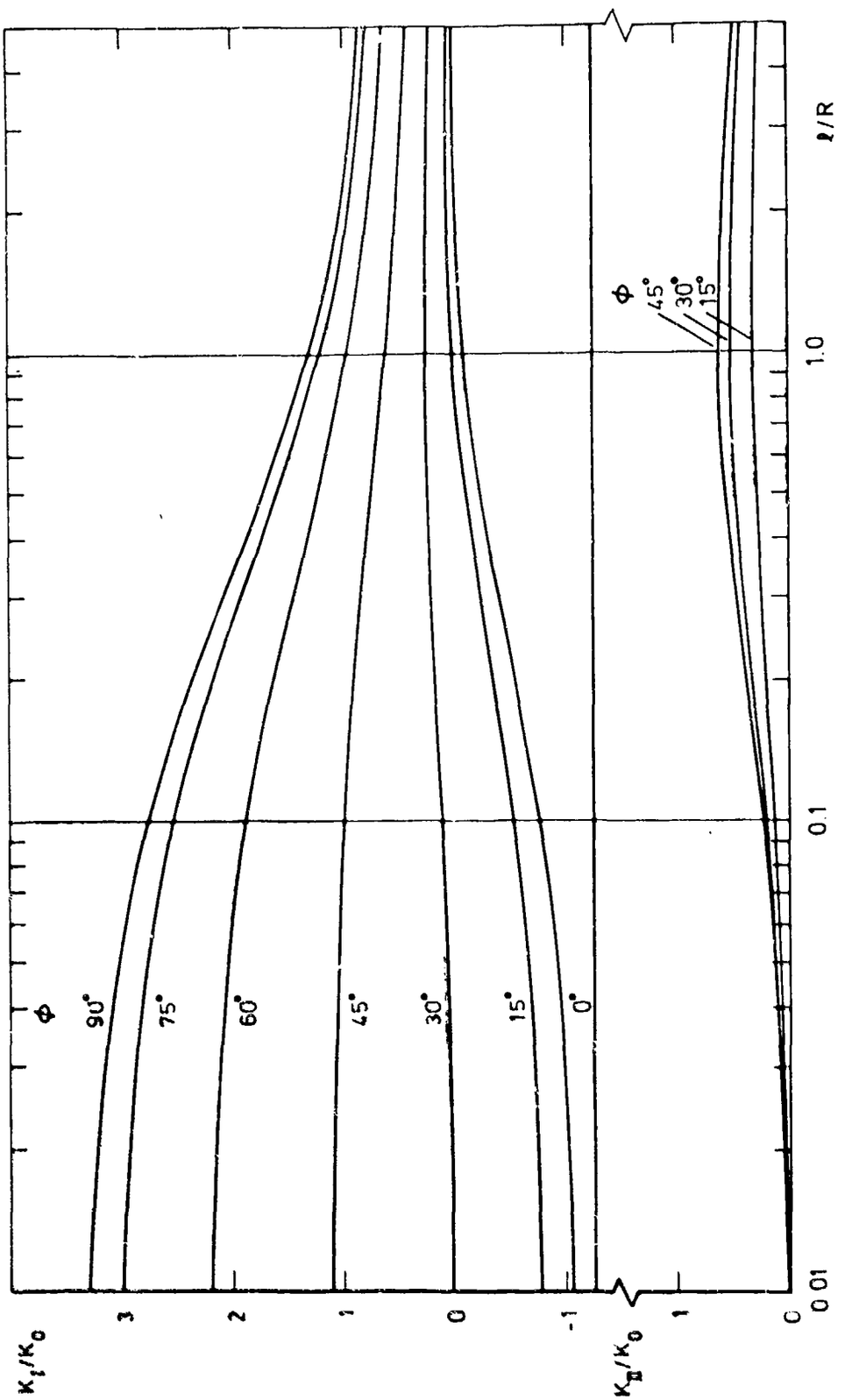

Fig 2 Opening-mode and sliding-mode stress intensity factors: uniaxial tensile stress

TR 81086

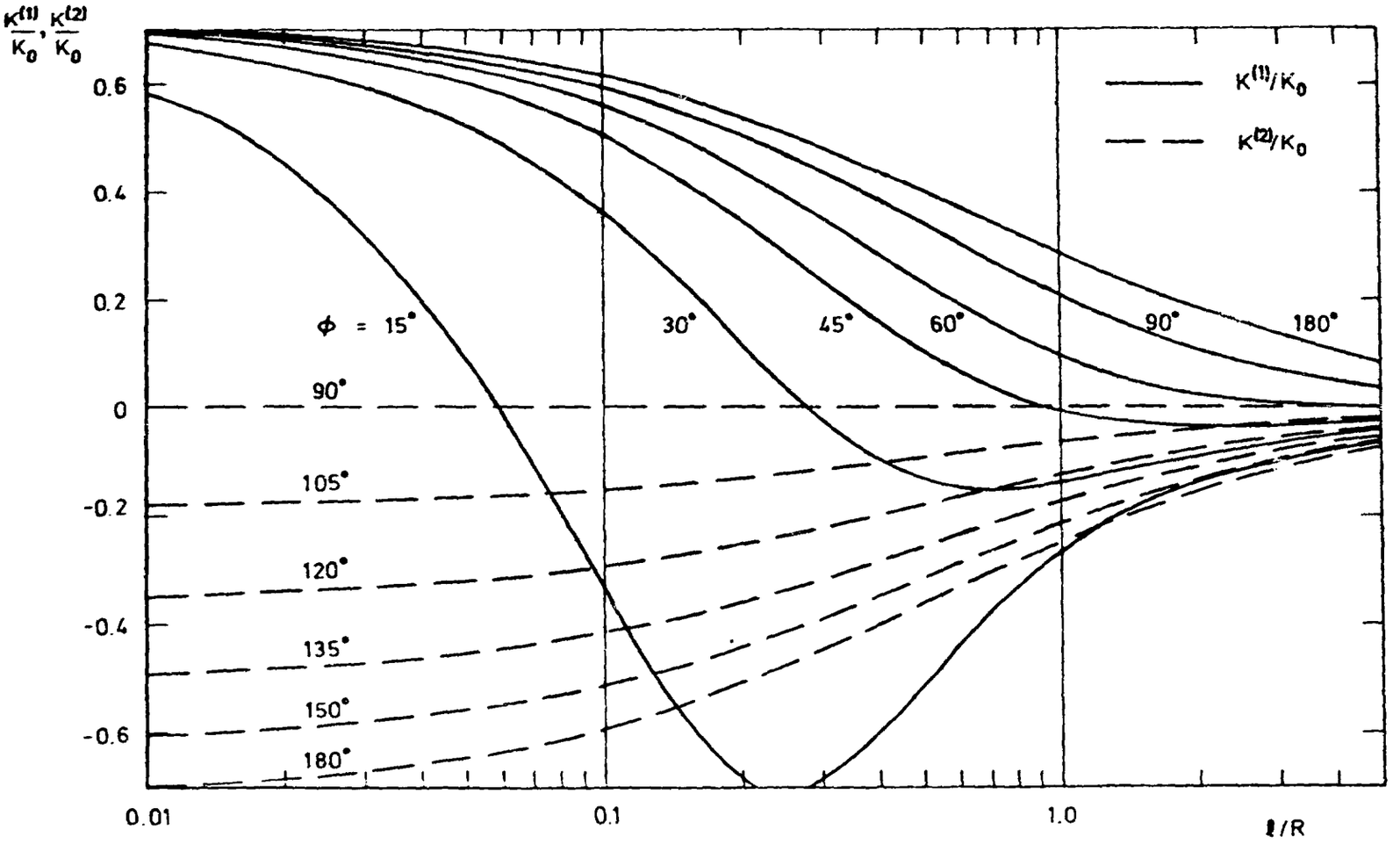

Fig 3 $K^{(1)}/K_0$ and $K^{(2)}/K_0$ components of opening-mode stress intensity factor: point load

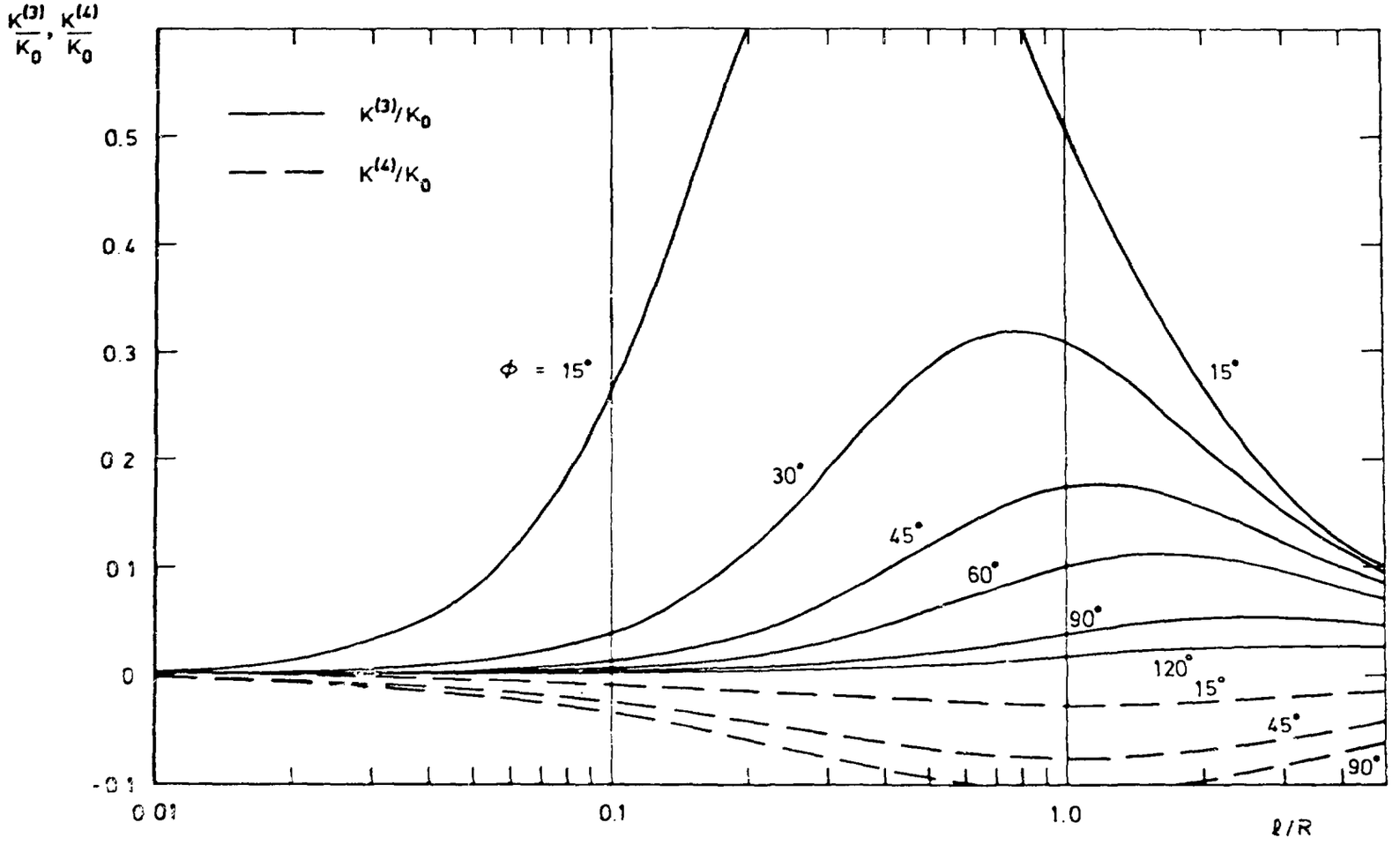

Fig 4 $K^{(3)}/K_0$ and $K^{(4)}/K_0$ components of sliding-mode stress intensity factor: point load

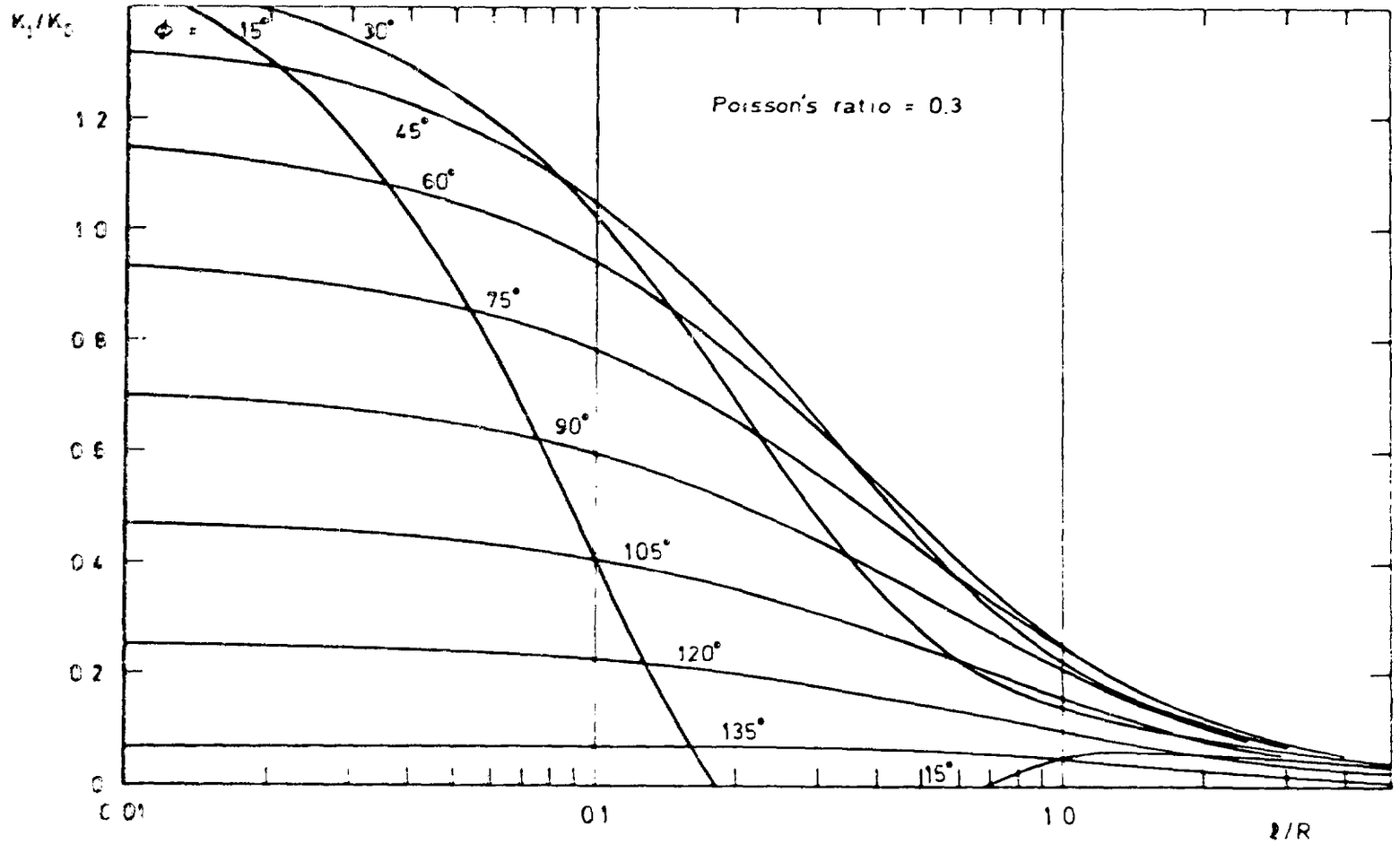

Fig 6 Opening-mode stress intensity factor: point load

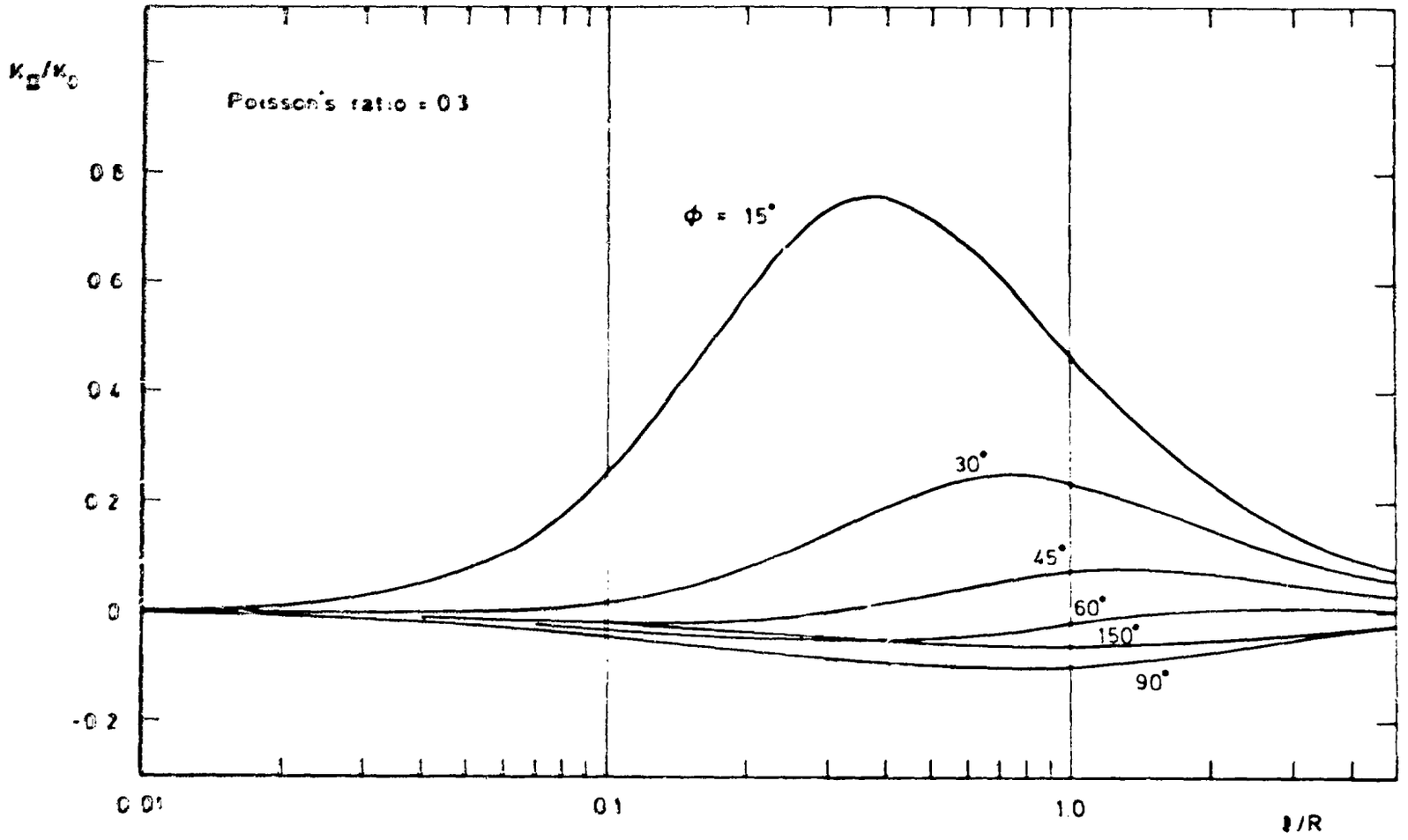

Fig 6 **Sliding-mode stress intensity factor: point load**

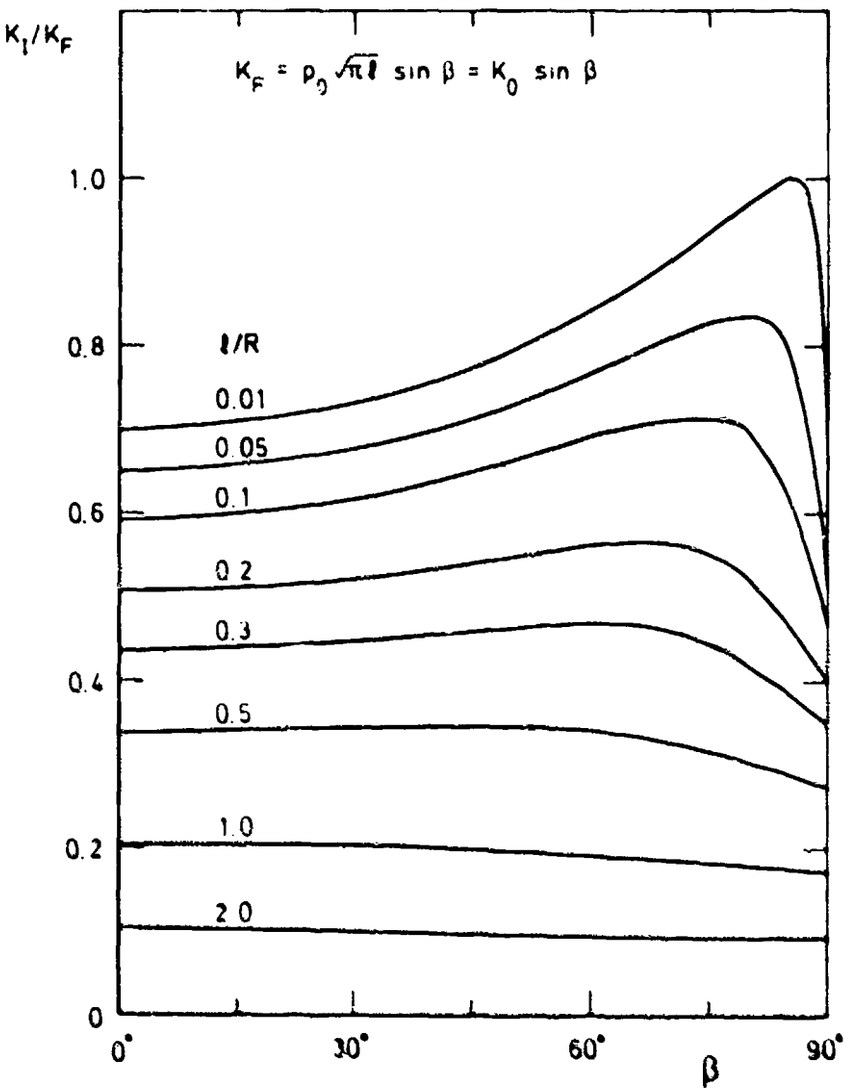

Fig 7 Opening-mode stress intensity factor: arc of uniform pressure

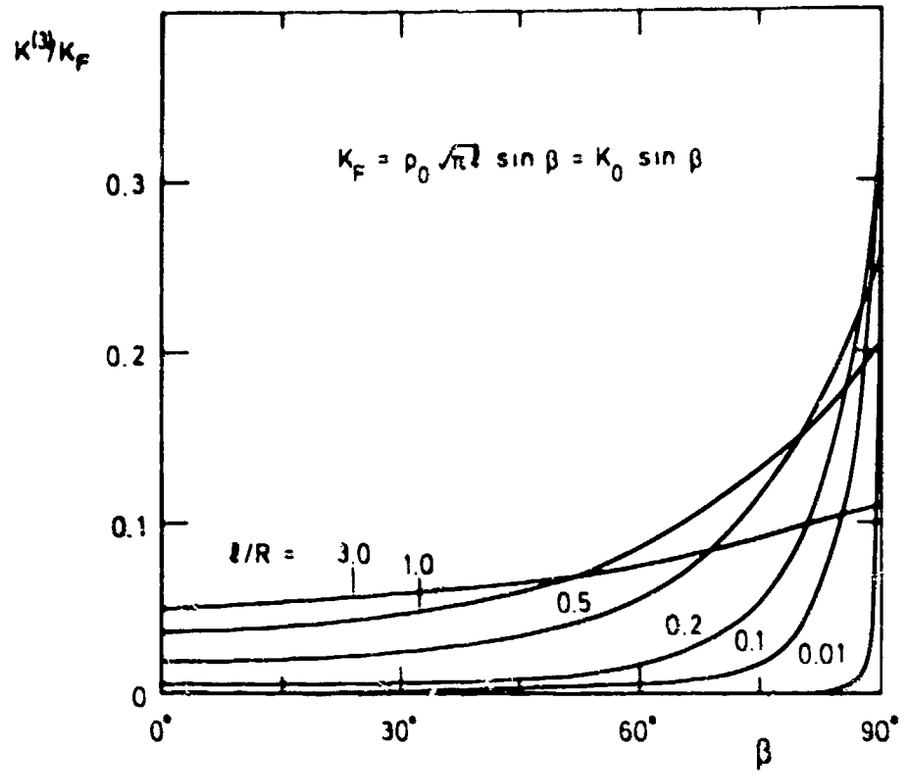

Fig 8a $K^{(3)}/K_F$ component of sliding-mode stress intensity factor: arc of uniform pressure

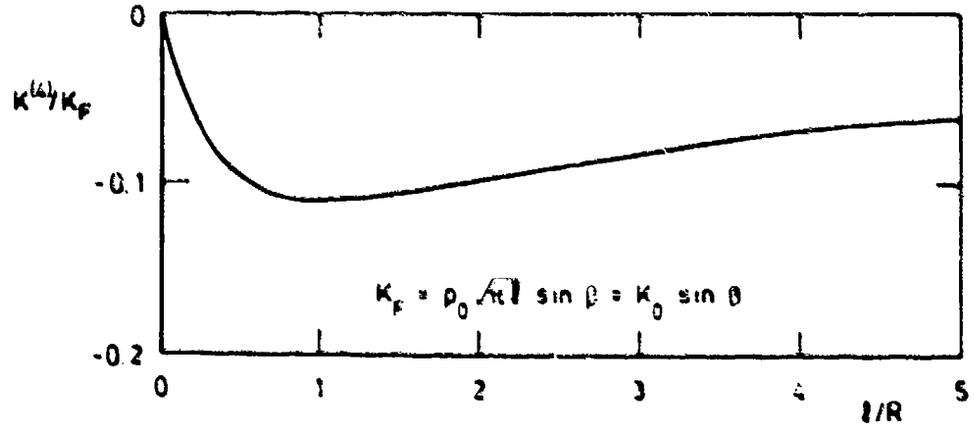

Fig 8b $K^{(4)}/K_F$ component of sliding-mode stress intensity factor: arc of uniform pressure

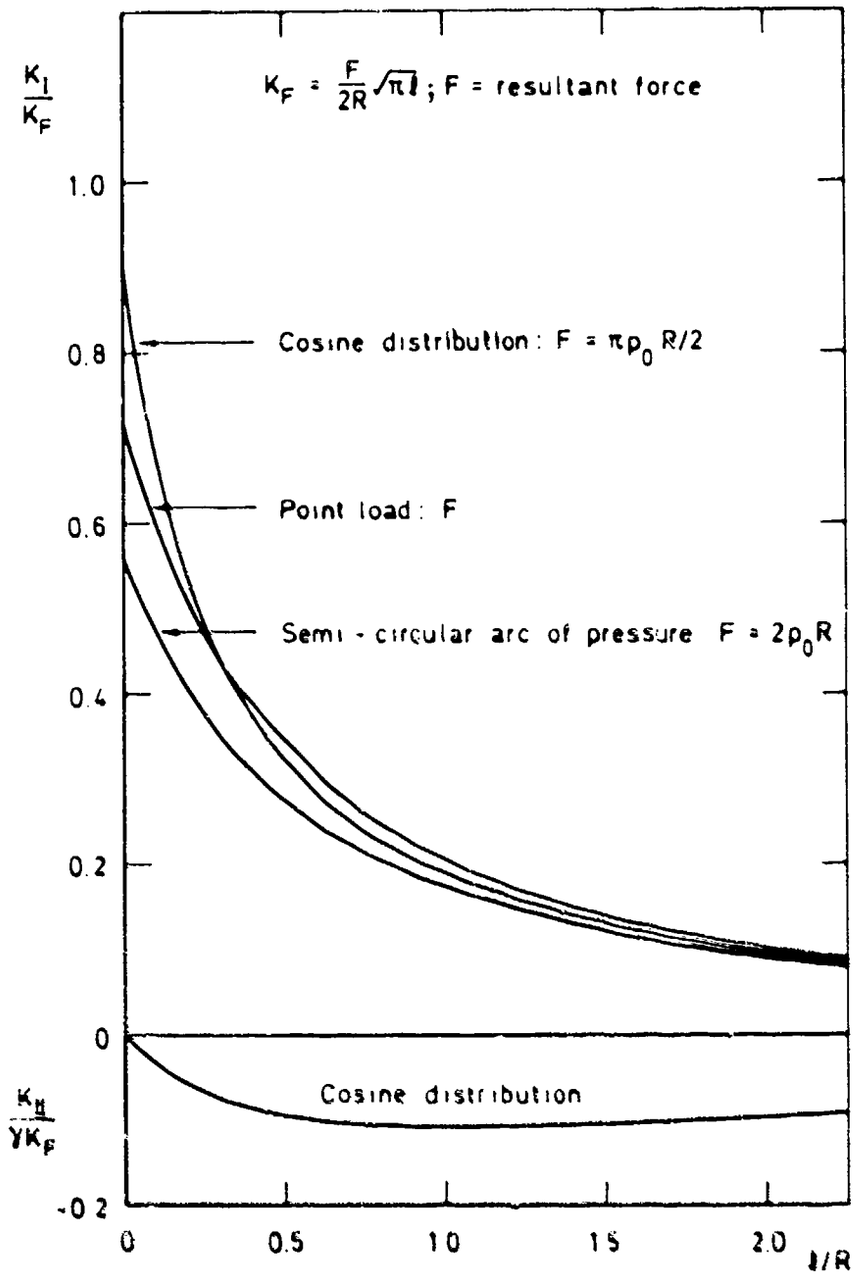

Fig 9 Opening-mode and sliding-mode stress intensity factors: distributions with equal resultant force

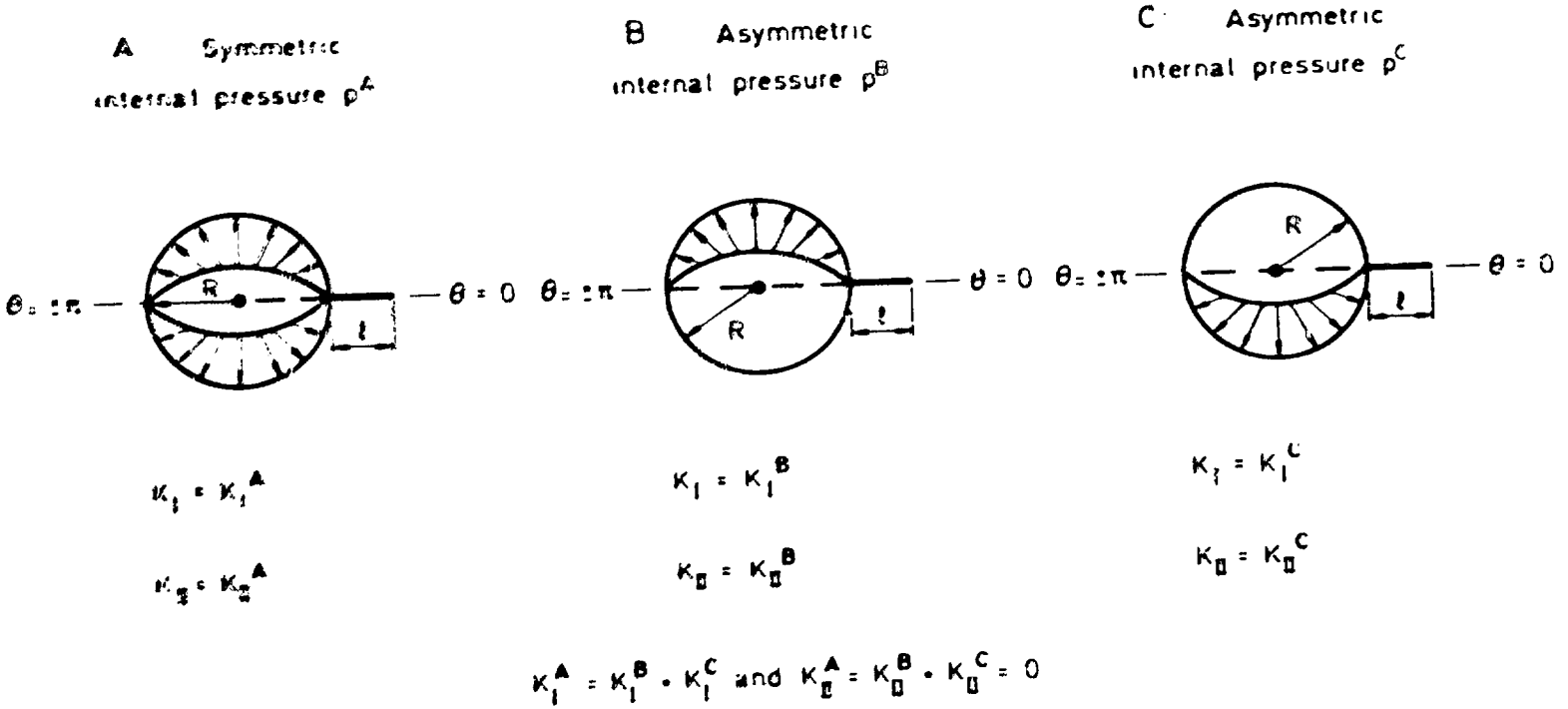

Fig 10 Superposition of two asymmetric loadings to form a symmetric loading.
($p^A = p^B + p^C$)

REPORT DOCUMENTATION PAGE

Overall security classification of this page

UNCLASSIFIED

As far as possible this page should contain only unclassified information. If it is necessary to enter classified information, the box above must be marked to indicate the classification, e.g. Restricted, Confidential or Secret.

1. DRIC Reference (to be added by DRIC)	2. Originator's Reference	3. Agency Reference	4. Report Security Classification/Marking
	RAE TR 81086	N/A	UNCLASSIFIED

5. DRIC Code for Originator	6. Originator (Corporate Author) Name and Location
7673000W	Royal Aircraft Establishment, Farnborough, Hants, UK
5a. Sponsoring Agency's Code	6a. Sponsoring Agency (Contract Authority) Name and Location
N/A	N/A

7. Title

Stress intensity factors for cracks at loaded holes

7a. (For Translations) Title in Foreign Language

7b. (For Conference Papers) Title, Place and Date of Conference

8. Author 1. Surname, Initials	9a. Author 2	9b. Authors 3, 4	10. Date	Pages	Refs.
Rooke, D.P.	Tweed, J.		July 1981	39	7

11. Contract Number	12. Period	13. Project	14. Other Reference Nos.
N/A	N/A		Mat 435

15. Distribution statement

(a) Controlled by – AD/XR via DRIC

(b) Special limitations (if any) –

16. Descriptors (Keywords) (Descriptors marked * are selected from TEST)

Cracks*. Holes. Stress intensity factors. Fracture mechanics.

17. Abstract

A method is described for obtaining the opening-mode and sliding-mode stress intensity factors for the tip of a crack at the edge of a circular hole with arbitrary loads on its perimeter. The method involves the solutions of a singular integral equation which arises from expressing the equations of elasticity in terms of Mellin transforms. In developing the method, four particular load distributions are considered: a uniform tensile stress remote from the hole; a point load on the perimeter of the hole; uniform pressure on an arc of the perimeter; a cosine distribution of pressure on the perimeter. It is shown that the stress intensity factor for a short crack is strongly dependent on the distribution of load around the hole; this has important implications for the estimation of fatigue lifetimes. A procedure is indicated for using some of the results to study arbitrary loads on the hole perimeter.

F5910/1